

Structure and Properties of BaO -B₂O₃ -Al₂O₃ -NaCl Glass System.

H. A. Silim

Grg, Physics Department, Faculty Of Science

Mansoura University, Mansoura 35516, El-Dakahlia, Egypt.

E-Mail: Hasilim @ Hotmail.Com

Barium aluminoborate glass of composition: xBaO-yAl₂O₃- (100-x-y) B₂O₃ -2yNaCl, with y = 3 and x = 3, 8, 13, 18 and 23 mol % were prepared, its structure and properties were also investigated. The structure was examined using Fourier Transform Infrared (FTIR) spectroscopy. The D C electrical conductivity and glass density were also measured. The analysis of the FTIR spectra revealed that there are seven absorption peaks with three quite active ones lying in the following regions: 1200 – 1600 cm⁻¹, 800 – 1200 cm⁻¹ and 600- 800 cm⁻¹ which are consistent with previous data reported by many authors. These peaks represent the absorption of the structure units that consists the glass matrix. The change in the position and relative area of these peaks demonstrates the structural modification accompanied with the change of the glass composition.

1.Introduction:

It is well known that the main structural units of the borate network which are [BO₃] triangles and [BO₄] tetrahedral, may form different super-structural units; boroxol and metaborate rings, metaborate chains, pentaborate, triborate, diborate and pyroborate. There are two types of [BO₃] triangles; the symmetric one with three bridging or non-bridging oxygen and the asymmetric one with one or two non-bridging oxygen [1]. Author [2] pointed out that aluminum atoms have mainly a tetrahedral coordination with respect to oxygen in barium and lead aluminoborate glasses. So it is not ruled out that the stretching vibrations of the Al-O in [AlO₄] groups can contribute to the absorption bands in the 800- 1200 cm⁻¹. Aluminum atoms in six-fold coordination can be detected from the absorption band in 400 – 600 cm⁻¹ regions. In the glass system of BaO-Al₂O₃ – B₂O₃, it was reported that [3-5] Al₂O₃ behaves as AlO₄ or AlO₆ units in the glass structure. It was also assumed that

aluminum ions enter the structure in the form of triclusters, where the triclusters consist of three tetrahedrals BO_4 and/or Al_2O_3 in the form of AlO_4 having an oxygen in common [5]. For the glass systems of $\text{MO}-\text{Al}_2\text{O}_3-\text{B}_2\text{O}_3$; (M = Sr, Ca and Ba) Owen [6] proposed that some of the M atom associate themselves with Al_2O_3 forming AlO_4 and the rest act with B_2O_3 producing BO_4 or non-bridging oxygen ions. Sakka [7] concluded that the ratio $\text{Al}_2\text{O}_3 / \text{CaO}$ affects on the glass structure where AlO_4 is dependent on B_2O_3 content. Pernice et.al [1] reported that the glass stability in the $\text{BaO}-\text{Al}_2\text{O}_3-\text{B}_2\text{O}_3$ system increases with respect to the devitrification process when Al acting as glass former.

In the present study the structure and properties of $\text{BaO}-\text{B}_2\text{O}_3$ glasses doped with 3 mol % of Al_2O_3 and 6 mol % of NaCl were investigated by FTIR spectroscopy, D C electrical conductivity and density studies are carried for different compositions of these glasses.

2. Experimental

2.1 Preparation of the glass samples

The glasses under investigation having the general formula: $x \text{BaO} - (100 - x - y) \text{B}_2\text{O}_3 - y \text{Al}_2\text{O}_3 - 2y \text{NaCl}$ with $y = 3$ mole % and $x = 3, 8, 13, 18$ and 23 mol % have been prepared using reagent-grade materials. The raw-materials: BaCO_3 , H_3BO_3 , Al_2O_3 and NaCl . A mixture of these materials in appropriate portions was melted in air in porcelain crucibles in an electric furnace in the temperature range from 1100 to 1300 °C with holding time of 2.5- 3 hours depending on the glass composition. The homogenised melts were cast into stainless steel moulds and subsequently cooled down to room temperature. X-ray diffraction patterns of the prepared glasses confirmed that they are amorphous.

The compositions of the studied glasses together with its melting time and annealing temperature are given in Table (1).

2.2 D C electrical conductivity

The D C conductivity measurements were carried out using polished samples of 1-2 mm thickness and coated with silver paste to serve as electrodes in the temperature range $270 - 450$ °C. The radius of the coated surface was of about 5 mm. The resistance of three replicates samples (for each composition) were measured using an Insulator Tester type TM14 with $10^3 - 10^{13}$ Ω ranges. The applied potential difference was 10 volt. The experimental error in determining the conductivity is expected to be $\approx \pm 5\%$ whereas the estimated error in the activation energy is less than 0.11 eV.

2.3 Density measurements

The densities were determined out using Archimedes' method with xylene as an immersion fluid. Three replicate samples of each glass composition were used to measure the density. The random error in the density measurements was estimated to be $\pm 0.05\%$. Density data are given in Table(1).

Table (1): Glass composition, activation energy, density. $\ln \rho_{400}$, melting time (hr) and annealing temp.($^{\circ}\text{C}$).

	BaO mol %	Al ₂ O ₃ mol %	B ₂ O ₃ mol %	NaCl mol %	Activatin energy (eV)	Density (gm.cm ⁻³)	$\ln \rho_{400}$ (Ω ..cm)	melting time (hr), annealing temp.($^{\circ}\text{C}$)
G10	3	3	88	6	1.684	1.195	23.52	2.5, 350
G11	8	3	83	6	1.366	1.755	25.19	2.5, 350
G12	13	3	78	6	1.400	2.011	24.82	2.5, 400
G13	18	3	73	6	1.295	2.036	25.522	2.5, 350
G14	23	3	68	6	1.316	2.239	25.95	2.5, 350

2.4 Fourier Transformation Infrared (FTIR)

The FTIR absorption spectra were recorded at room temperature in the range 400 – 4000 cm⁻¹ using Mattson 5000 FTIR spectrometer with a spectral resolution of 2 cm⁻¹. A KBr pellets technique was used where 10 mg of each sample is mixed with 1000 mg of KBr in an agate mortar. From this stock, 200 mg were then pressed into pellets of 13 mm diameter. The spectrum of each sample represents an average of 20 scans, which were normalised to the spectrum of blank KBr pellet; i.e. a pure KBr spectrum was subtracted from each glass spectrum. Also, the spectra were corrected to the background and dark currents.

3. Results and discussions:

3.1 Analysis of FTIR spectra

The infrared absorption spectra of the studied glasses are shown in Fig.(1), where all the spectra are shifted upwards for the sake of clarity. In this figure x = 3, 8, 13, 18 and 23 mol % of BaO. Fig. (2) represents an example of the deconvoluted infrared spectrum for BaO = 13 mol %. The Gaussian shape was found to be the best fit obtained the IR bands.

The peak centre C and the relative area R of the component bands of the FTIR spectra are listed in Table (2).

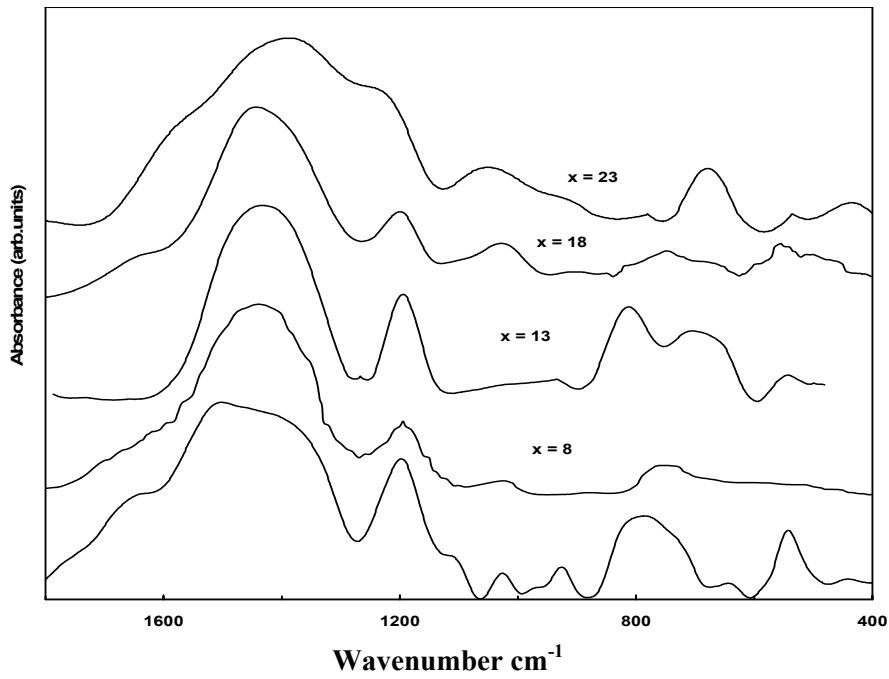


Fig. (1): FTIR absorption spectra for the studied glasses with $x = 3, 8, 13, 18$ and 23 mol % of BaO. Successive spectra have shifted upward.

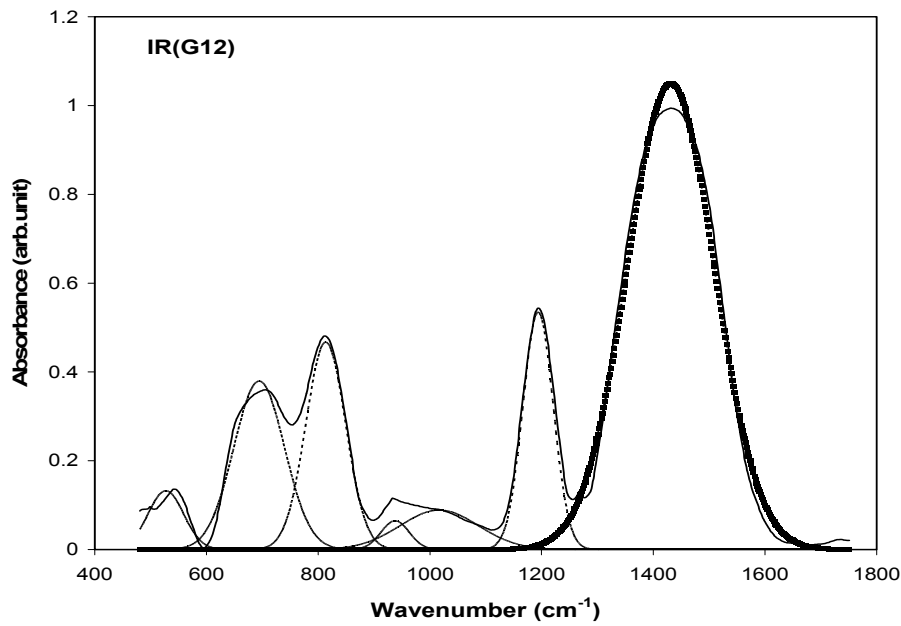


Fig. (2): Deconvolution result for $13 \text{ BaO} - 3 \text{ Al}_2\text{O}_3 - 78 \text{ B}_2\text{O}_3 - 6 \text{ NaCl}$, experimental absorption spectrum (solid) and computer bands (dashed lines).

Table (2): Peak centre and relative area for the studied glasses. [C: Peak centre, R: Relative area]

G10	C	537.5	777.6	933.1	1196.1	1360.1	1487.1	1653
G10	R	0.0451	0.1149	0.0142	0.1536	0.1713	0.3155	0.1855
G11	C	622.8	752.4	898.2	1047.1	1194.8	1433.4	1628
G11	R	0.0591	0.0316	0.0027	0.0313	0.0958	0.6008	0.1780
G12	C	527.3	694.4	813.5	937.7	1016.8	1193.8	1431.1
G12	R	0.0274	0.1213	0.1173	0.0114	0.0437	0.1023	0.5768
G13	C	494.5	557.7	747	1041.4	1201.1	1431	1662.2
G13	R	0.037	0.0185	0.0921	0.0942	0.0909	0.6066	0.0606
G14	C	433.8	678.5	963	1049.2	1218.8	1393.8	1587.1
G14	R	0.0396	0.0595	0.0995	0.0503	0.07	0.6718	0.0596

According to Krogh-Moe's [8] model, the structure of the boron oxide glass consists of a random network of planer BO_3 triangles with certain fraction of boroxol rings. The FTIR spectra of the studied glasses, Fig. (1), are characterised by seven absorption regions. These regions correspond to the modes of borate network are seen to be active in three infrared spectral regions which are similar to those reported on alkali borate [8,9,10] and barium and aluminoborate glasses [2,11]

These regions are: (1) $1200 - 1700 \text{ cm}^{-1}$ is due to the asymmetric stretching of the B – O band of triangle $[\text{BO}_3]$ units, (2) $800 - 1200 \text{ cm}^{-1}$ is due to the B – O stretching vibration of tetrahedral $[\text{BO}_4]$ units and (3) $600 - 800 \text{ cm}^{-1}$ due to bond bending vibration of B – O – B groups [12,13,14].

In pure B_2O_3 glass, the absorption peak at 806 cm^{-1} wave number is a characteristic band of boroxol ring. In the present glass system the absence of this peak; except in G13; indicates the absence of boroxol ring formation, ultimately it consists of BO_3 and BO_4 groups. The band around 1360 cm^{-1} in G 10 is assigned to B – O stretching vibration of triagonal $[\text{BO}_3]$ unites in metaborate, pyroborate and orthoborates [15] where the bond between BO_3 and BO_4 is slightly broken. The band at wave number $\leq 550 \text{ cm}^{-1}$ is due to the vibration of the modifier cations Na^+ . The boroxol ring appears at 778 cm^{-1} wave number, the absorption band at 1196 cm^{-1} wave number are characterising of pentaborate, which consists of one BO_4 and three BO_3 . The band at 1487 cm^{-1} is assigned to the metaborate chains [10], i.e. formation of BO_4 on the expense of BO_3 with nonbridging oxygen [NBO]. The band at 1653 cm^{-1} arises from B – O stretching vibration of triangle $[\text{BO}_3]^{-3}$ unites [8,9,16,17] where the bond between BO_4 and BO_3 is highly broken.

In G11 spectrum, the band at 623 cm^{-1} is assigned to the pentaborate while the bands at 752 , 1433 and 1628 cm^{-1} are similar to the bands at 778 , 1487 and 1653 cm^{-1} of G10, respectively. The bands around 1047 cm^{-1} and 1195 cm^{-1} could be referred to from pentaborate chains.

In G12, the band at 1431 cm^{-1} is similar to that at 1433 cm^{-1} of G11 sample, while those at 694 cm^{-1} and 1194 cm^{-1} can be assigned to the pentaborate. The absorption band at 938 cm^{-1} is due to the diborate network [15].

In glass sample G13, the bands at 747 , 1041 and 1201 cm^{-1} are referred to the pentaborate, whereas those at 1431 cm^{-1} and 1662 cm^{-1} are similar to those at 1433 cm^{-1} in G11 or 1487 cm^{-1} and 1653 cm^{-1} in G10. The band at 558 cm^{-1} is assigned to the vibration of the modifier cation as in G10 sample [15].

In G14, the absorption peaks at 1394 cm^{-1} and 1587 cm^{-1} are similar to those at 1360 cm^{-1} and 1487 cm^{-1} of glass G10, respectively. The peaks at 679 , 1049 and 1219 cm^{-1} are due to the formation of pentaborate while that at 963 cm^{-1} is representing diborate [15].

The independence of the IR data (peak position and relative area) for the studied glass may be due to the complex modification of the glass matrix upon changing the composition. Starting with G10, it has 88 mol % B_2O_3 and the rest are BaO, Al_2O_3 and NaCl. The glass matrix will be modified with 12 mol % of three different oxides that have different roles in the glass matrix. Ba^{++} ions will act as glass modifier and convert the BO_3 triangles into BO_4 groups. Al_2O_3 plays a dual role in borate matrix as glass modifier when it added to B_2O_3 with low concentration and glass former for high concentrations. Substitution of BaO for B_2O_3 in the studied glass seems to lead to the conversion in the direction of the NBO's formations [8, 9, 16, 17].

This can be seen clearly from the strong overlapping of the BO_3 bands in the region of $1200 - 1700\text{ cm}^{-1}$. The other absorption bands seem to be compositional dependence.

3.2 D C conductivity and Density

The conductivity data showed quite agreement with Arrhenius' equation:

$$\sigma = \sigma_0 \exp(-E/RT) \quad (1)$$

Where, σ_0 is the pre-exponential factor, E is the activation energy for the ionic conduction, R is the universal gas constant and T is the absolute temperature in

K. DC electrical conductivity for all the glass samples is measured as a function of temperature. Fig. (3) shows that the plot of $\ln \rho$ versus $1000 / T$ is a linear relation and the values of $\ln \rho$ at any fixed temperature (400°C) increases with increasing BaO concentration except at 8 mol %. The calculated activation energies from this figure are given in Table (1). A plot of activation energy versus BaO composition along with $\ln \rho_{400}$ ($\Omega \cdot \text{cm}$) are given in Fig.(4).

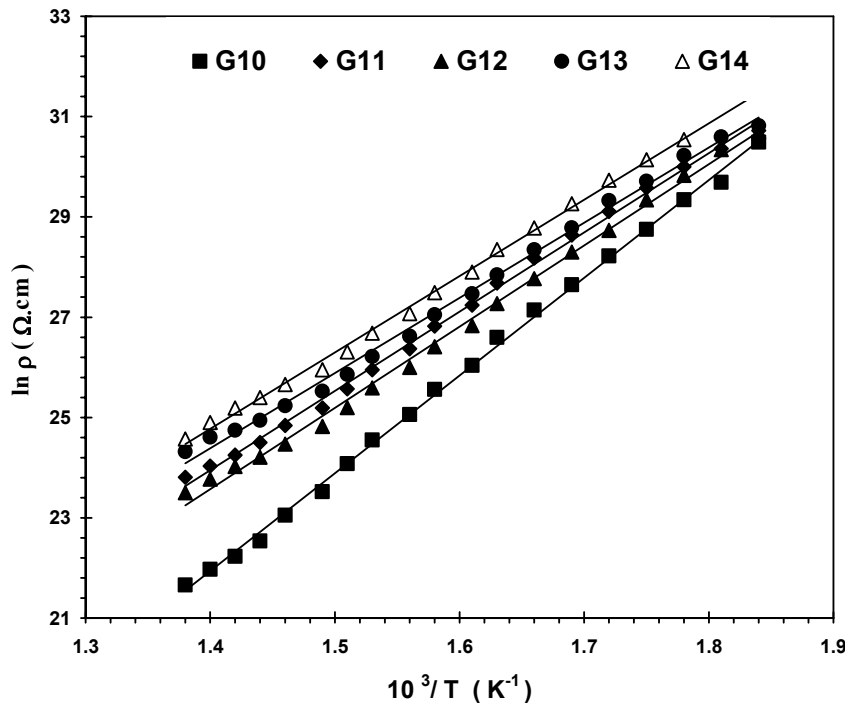


Fig. (3): Change of the natural logarithm of electric resistivity $\ln \rho$ for the investigated glasses versus $1/T$.

In the glasses under investigation it is very known that B_2O_3 and Al_2O_3 in form of AlO_4 are plying as glass former, BaO enters the network as modifier and Na^+ as charge carriers. Since NaCl is constant, thus the ratio $\text{NaCl} / \text{B}_2\text{O}_3$ increases this means that Na^+ is slightly increases and an improving in the conductivity could be observed which caused the activation energies to be decreased. This means that BaO will act as modifier. It is known that the introducing one molecule of BaO into B_2O_3 converts two BO_3 units into two BO_4 units [18]. This leads that the mobility of the charge carries species increases with increasing transformation rate of BO_3 to BO_4 . This process continues up to about 33 mole % of BaO where the number of BO_4 units reaches its maximum value and NBO starts to be formed at $\text{BaO} > 33 \text{ mol } \%$,

which is inconsistent with the results of the present study, where the maximum value of BaO = 23 mol %. This means that BaO is not considered as a pure charge carries as Na⁺ but may play the role of both carriers and modifier. The formation of NBO ions leads to decreasing the height of the potential for Na and increasing the Ba mobility.

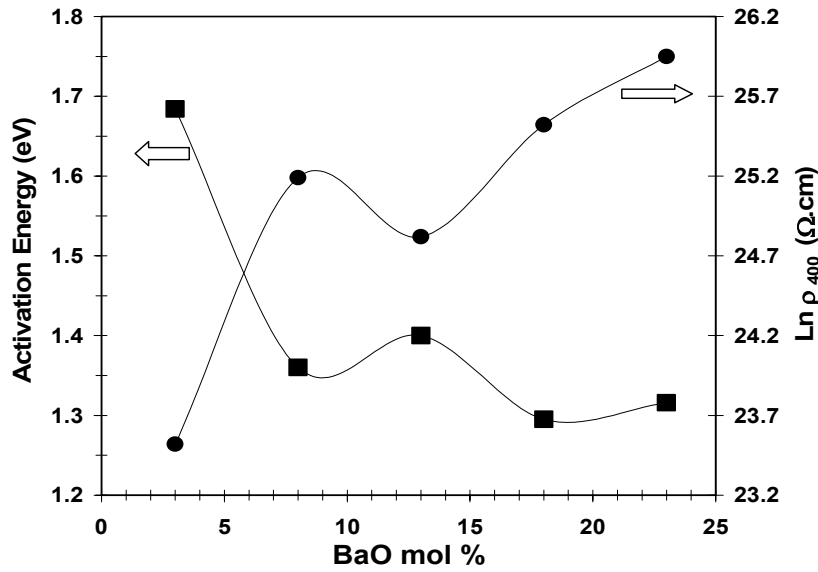


Fig. (4): Change of both the activation energy for the electrical conduction and the natural logarithm of Ln ρ at 400 °C versus the BaO content.

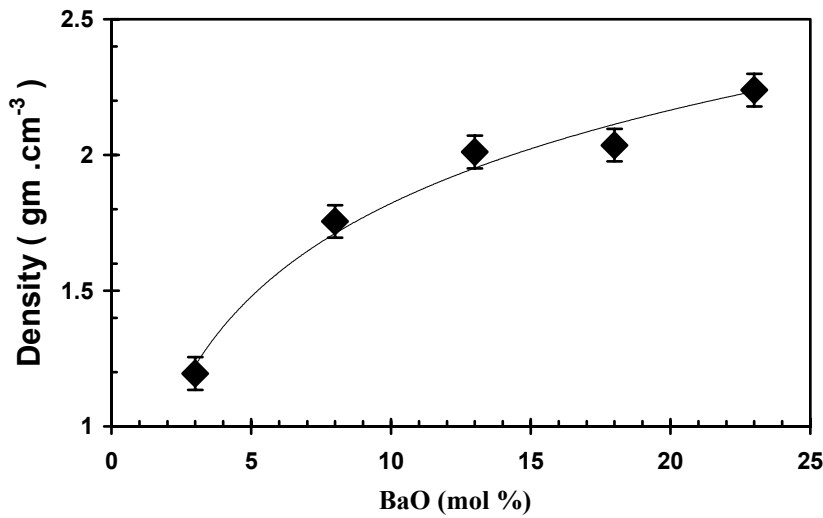


Fig. (5): Change of density with BaO content in the studied glasses. Density data are given in Table (1). The relation between the density (gm / cm³) data and BaO content is shown in Fig. (5), where the density

increases as BaO mol % is increased. This means that there are some enhancement existence of the glass as B₂O₃ decreases.

4. Conclusion:

The FTIR spectroscopy for the investigated glasses showed that the Deconvolution of effective range (400 – 2000 cm⁻¹) revealed that there are three active regions that are quite consistent with previous data reported by other authors. These regions are: 600- 800 cm⁻¹, 800 – 1200 cm⁻¹ and 1200 – 1700 cm⁻¹. The D C electrical conductivity indicates that the activation energy decreases as the ratio NaCl / B₂O₃ increases and the possibility for nonbridging oxygen (NBO) to be formed is acceptable this is due to the constancy of Al₂O₃ and NaCl for all glasses. NBO ions in borate network enhance the mobility of the charge carries. The density results lead one to believe that the enhancement of glasses increases as B₂O₃ decreasing.

5. Acknowledgements

I would like to thank Prof. G. El-Damrawi and Prof. Y. M. Moustafa, my colleagues in GRG, Physics Department, Mansoura University, for their useful comments, reviewing the manuscript and their assistance through out this work.

References:

1. P. Perince, S. Esposito, A. Aronne and V. N. Sigaev, *J. Non-Cryst. Solids* **258**, 1 (1999) .
2. V. Z. Kreitsberga, V. G. Chekhovskii, A. P. Sizonenko, Yu. Ya. Keishs, S. E. Redala and P. G. Pauksh, *Fiz. Khim Stekla* **17**, 953 (1991) .
3. H.Scholze, “*Glass : Nature, Structure and Properties*”, Springer, New York, (1991)
4. J.E. Shelby, *Introduction to “Glass Science and Technology”*, The Royal Society of Chemistry, Combridge, (1997).
5. A.E. Owen, *Phys. Chem. Glasses* **2**,152 (1961) .
6. Y. Naruse, A. Abe, Takami, *Yogyo- Kyokai-Shi* **79**, 225 (1971) .
7. S. Sakka, *Yogyo- Kyokai- Shi* **85**, 299 (1977).
8. Krogh Moe, *Phys. Chem. Glasses* **6**, 46 (1965).
9. E. I. Kamitsos, M. A. Karakassides, and G. D. Chyrssikos, *Chem. Phys. Glasses* **91**, 1073 (1987).
10. E. I. Kamitsos, A. P. Patsis, M. A. Karakassides and G. D. Chyrssikos, *J. Non-Cryst. Solids* **126**, 52 (1990) .

11. V. G. Chekhovskii, Yu. Ya. Keishs and Yu. A. Petrov, *Fiz. Kim. Stekla* **14**, 150 (1988).
12. P. Perince, S. Esposito and A. Arone, *Phys. Chem. Glasses* **39**, 222 (1998).
13. P. Perince, A. Arone and A. Marrotta, *Mater. Chem. Phys.* **30**, 195 (1992).
14. P. Perince, A. Arone and, M. Cataura, *Phys. Chem. Glasses* **37**, 134 (1996).
15. V. G. Chekhovskii, *Fiz. Kim. Stekla* **11**, 24 (1985) .
16. Y. M. Moustafa, H. Doweidar and G. El-Damrawi, *Phys.Chem. Glasses* **35**, 104 (1994).
17. E. I. Kamitsos, M. A. Karakassides and G. D. Chyrssikos, *Phys. Chem. Glasses* **28** (5), 203 (1987).
18. P. J. Bray, *Borate Glass, Structure, Properties, Applications*, ed.I. D. Pye, V. D. Frechette, N. J. Kreidle (Eds), Plenum, New York (1978).